Magnetism of Co-doped ZnO thin films

Milan Gacic, Gerhard Jakob, Christian Herbort, and Hermann Adrian
Institute of Physics, University of Mainz, Staudinger Weg 7, D-55099 Mainz, Germany

Thomas Tietze, Sebastian Brück, and Eberhard Goering
Max-Planck-Institute for Metal Research, Heisenbergstrasse 3, 70569 Stuttgart, Germany
(Received 27 November 2006; revised manuscript received 1 March 2007; published 22 May 2007)

We have investigated magnetic and transport properties of 5% Co-doped and undoped ZnO thin films deposited on *r* plane Al_2O_3 substrates by pulsed laser deposition. The Co doped films showed paramagnetic and ferromagnetic behavior as well as a high magnetoresistance and a small anomalous Hall effect. In a range of 0 to 5 T at low temperatures we observed a double sign change of the magnetoresistance. For undoped ZnO films, prepared by the same conditions, only a negative MR was observed, but surprisingly also a very small anomalous Hall effect. We explain our results by applying a semiempirical fit consisting of a positive and a negative contribution to the magnetoresistance. Using x-ray magnetic circular dichroism we investigated element specific magnetic moments in Co-doped laser ablated ZnO films. As the Co atoms show a paramagnetic behavior, we attribute the ferromagnetism to a spontaneously spin impurity band induced by oxygen vacancies and defects due to the transition metal doping and/or interface stress to the substrate.

DOI: 10.1103/PhysRevB.75.205206 PACS number(s): 75.50.Pp, 75.47.−m, 87.64.Gb, 85.75.−d

I. INTRODUCTION

Diluted magnetic semiconductors are semiconducting materials doped with magnetic ions such as Co or Mn and have attracted much interest in the last years because of their potential application in spintronics. The common objective is to synthesize a semiconductor with spin polarized charge carriers. The idea is that localized magnetic moments couple with the charge carriers without changing the semiconducting behavior of the base material or leading to a formation of metallic phases or clusters. Therefore the doping concentrations are usually below 10%. For practical applications it is necessary to have both *n*- and *p*-type conductors as well as ferromagnetism above room temperature. The first *p*-type DMS were realized with GaAs and InAs doped with a few percent of Mn.[1] These compounds show ferromagnetic ordering and also some impressive effects such as electrically controlled magnetism,[2] but with a Curie temperature (T_C) well below room temperature they are not suitable for practical applications. Calculations from Dietl *et al.*,[3] founded on hole mediated ferromagnetism, showed that *p*-type ZnO based diluted magnetic semiconductors should have a T_C above room temperature. Unfortunately ZnO is usually *n* doped and it is very difficult to establish *p* doping. Nevertheless some groups have found room temperature ferromagnetism in TM doped *n*-type ZnO (Refs. 4–6) and also other oxides,[7] while others contradict these findings.[8] The results are controversial and the reproducibility is very bad, so it is still not clear if the ferromagnetism is intrinsic or just due to some external impurities, metallic phases, or clusters. Without doubt the preparation method seems to play an important role. Most groups focused on ZnO and TiO_2 compounds, but there are also other reports where SnO_2 (Ref. 9) or Cu_2O (Ref. 10) are successfully used as base materials. Nevertheless ZnO has its advantages as it is a transparent direct wide bandgap semiconductor with a large exciton binding energy which allows it to be used not only for spintronic but also for magnetooptical devices and short wavelength light emitters. On this account we focus our work on 5% Co-doped ZnO thin films and try to find out the origin of the reported ferromagnetism. One way we exploit in order to distinguish between intrinsic ferromagnetism and impurities is to analyze transport properties such as magnetoresistance and Hall effect. Here we find a distinct low temperature magnetoresistance behavior of the ferromagnetic Co-doped films compared to the undoped films. The other method we apply is the investigation of element specific magnetic properties, which are evident in x-ray magnetic circular dichroism (XMCD) of the Co-absorption lines. We present experimental results showing that long range magnetic order is seemingly absent in the transition metals while a ferromagnetic moment is present, possibly due to a spontaneously spin split impurity band induced by the defect structure of the laser ablated $Zn_{0.95}Co_{0.05}O_x$ films.

II. EXPERIMENTAL

As some reports conclude that the ferromagnetism in ZnO is induced by defects as oxygen vacancies (Ref. 11) we tried to adjust our preparation conditions accordingly. All samples were prepared by pulsed laser deposition at 0.1 mbar argon pressure. We used a KrF laser with a wavelength of 248 nm, an energy density of 1 to 5 J/cm^2 and a repetition rate of 5 Hz. As a substrate we used 5×5 mm *r*-cut (1-102) Al_2O_3. For target preparation powders of ZnO and Co_2O_3 were mixed together, pressed and sintered for 12 h at 1000 °C in air. The distance between target and substrate was 45 mm. At a temperature of 600 °C we deposited with a rate of 5 nm/min. To avoid external impurities from the surface of the sample holder we covered it with a small molybdenum plate. We also used only nonmagnetic titanium tweezers so that there should not be any magnetic impurities on the edges or the bottom of the substrate. Our films were greenish and transparent and the thickness was between 20 and 120 nm.

Thickness and epitaxy were determined by x-ray diffraction. We used a transmission electron microscope (TEM) to investigate the crystal structure of the film especially at the interface and to look for possible Co clusters. The magnetic measurements were done by superconducting quantum interference device (SQUID) and vibrating-sample magnetometer (VSM). Because of the small absolute magnetic moments in the range of 5×10^{-6} to 5×10^{-5} emu we had to carefully subtract background signals from measuring stick and substrate, and also device dependent drifts had to be taken into account. We found that our substrates have a small ferromagnetic impurity below 3×10^{-6} emu and a paramagnetic one below 1×10^{-5} emu. For transport measurements we used a Hall geometry, patterned by standard UV lithography, which allows us to measure magnetoresistance and Hall effect using the same pattern. To improve the signal to noise ratio we sputtered ohmic gold contacts before. The contacts were annealed for 30 min at 700 °C in vacuum. For Hall measurements we reversed current and magnetic field directions in order to eliminate thermovoltages and magnetoresistive contributions. The x-ray magnetic circular dichroism (XMCD) and x-ray absorption spectroscopy (XAS) experiments were performed at the synchrotron BESSY II, in order to measure local atomic magnetic moments and to check the local chemical environment, respectively. All XMCD and XAS spectra were recorded in the total electron yield mode at the new high resolution bending magnet beamline PM III at Bessy II with an energy resolution $E/\Delta E=5000$. We used a new superconducting magnet system, providing fast field switching in less than 6 sec at ±2 T. All spectra have been measured in an applied magnetic field up to 2 T, which has been flipped at each energy data point. This provides a sensitivity of the XMCD signal up to 10^{-6} respective to the full absorption signal (room temperature and nondiluted bulk material), just at the pure photon statistics of the absorption process itself. This very high sensitivity allows the investigation of paramagnetic XMCD spectra at the Co $L_{2,3}$ edges down to about $10^{-4}\mu_B$.

III. RESULTS AND DISCUSSION

A. Structural properties

The XRD spectrum of our samples shows only the ZnO (110) peak in wurtzite structure and the substrate peaks (Fig. 1). No other phases were observed. The in plane orientation was measured with a four circle diffractometer. The *c* axis of the ZnO is oriented perpendicular to one hexagonal axis of the substrate, while both are parallel to the substrate surface. Though the film is growing epitaxially its quality is not perfect. The growth direction of the film crystal is sometimes slightly tilted relative to the substrate, which could be proven by TEM images (Fig. 2). The first 2 nm of the film are even strongly distorted, with higher thickness epitaxial strains relax. The atomic planes of the film at the interface resemble rather a distorted ZnO than a secondary phase. Further TEM investigations could not reveal any clusters in the crystal, though one cannot exclude them definitely by this method. The film composition was determined by EDX, thus the Co concentration in our samples was between 5 and 7%, showing a slight enrichment of Co in the films compared to the nominal value.

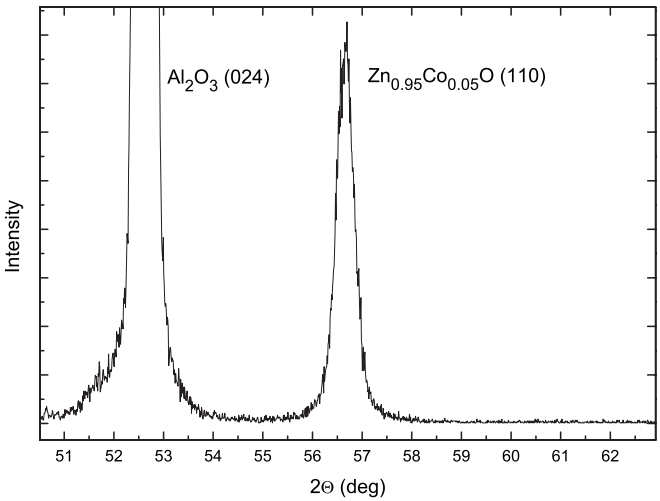

FIG. 1. XRD peak of ZnO in 110 direction. Film thickness was 25 nm. No other phases were observed.

B. Magnetic properties

Magnetization (M) versus field (H) measurements at room temperature showed a clear presence of ferromagnetism in our samples (Fig. 3). The samples showed no thickness dependence with respect to the ferromagnetic moment. However, the ferromagnetic magnetization was extremely sensitive to the preparation conditions. The magnetization varied between 2 to 20 emu/cm^3, which is

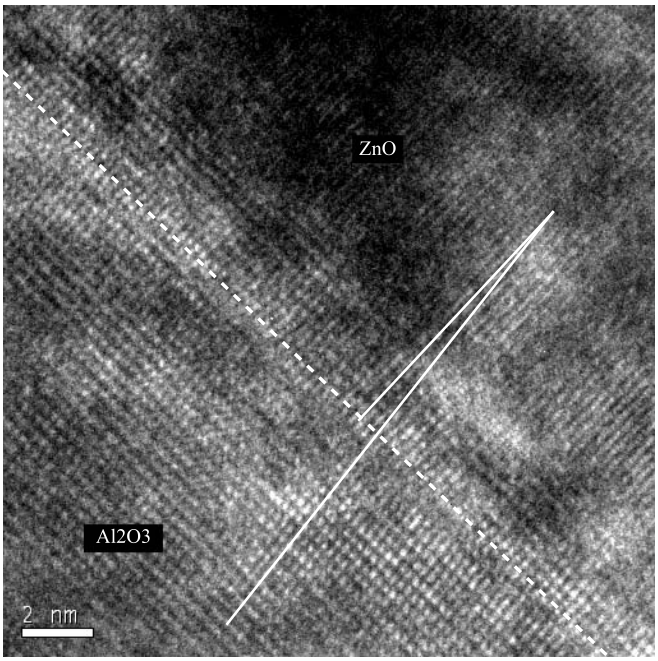

FIG. 2. TEM picture of the ZnO/Al_2O_3 interface (dashed line). The film is not growing very well on this substrate. As one can see the first 2 to 5 nm are very distorted. Due to that the lattices are slightly (up to 3°) tilted relative to each other.

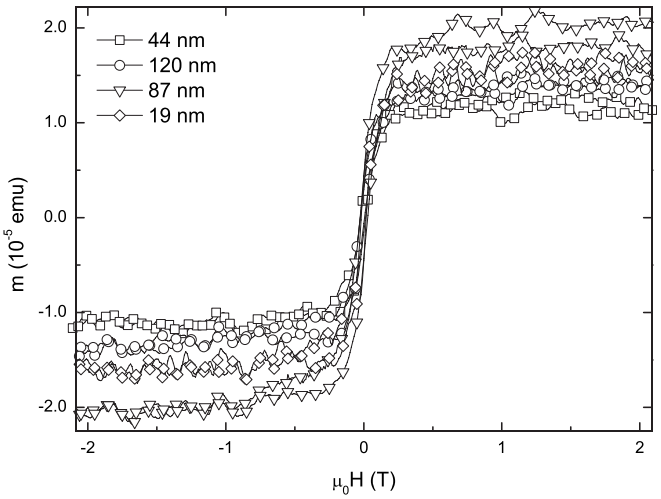

FIG. 3. VSM curves of $Zn_{0.95}Co_{0.05}O$ thin films for different thicknesses at RT. Background signals from substrate and measuring stick were subtracted as well as the paramagnetic contribution. We could not find a reproducible correlation between magnetic moment and film thickness.

equivalent to 0.1 to 1 Bohr magneton per Co. SQUID measurements show a remanence which is about 10% of the saturation magnetization and a coercitivity field of 100 Oe at 300 K. Low oxygen pressure and low laser energies seem to be beneficial for the magnetism which strengthens the presumption that defects are essential for ferromagnetic ordering. Besides that we could not find any other reproducible dependencies on the preparation parameters concerning the ferromagnetic properties. High field and low temperature VSM measurements showed that besides the ferromagnetic moment there is also a paramagnetic contribution which can be much higher than the ferromagnetic one, whereas the paramagnetic moment scales with the thickness in contrast to the ferromagnetic contribution. An example of such a measurement is shown in Fig. 4. A measurement of a bare substrate and sample holder was performed for each temperature and subtracted from the sample data. Quantitative VSM calibration was performed with a pure Ni-foil of the same shape as the sample. In the top of Fig. 4 we show the experimental curves measured at different temperatures. The ferromagnetic contribution shows no obvious temperature dependence, but is nearly identical for all temperatures. In the paramagnetic contribution a crossover from a linear magnetic field dependence at higher temperatures above 15 K to a curved low temperature behavior is visible. Indeed a simulation of the expected magnetic moment of paramagnetic Co^{2+} atoms in crystal field quenching orbital momentum ($J=S=1.5$; g factor=2) yields very good agreement. The temperature and field dependence is calculated with the Brillouin function and added to a constant ferromagnetic contribution. While the curvature is a single ion property, the signal size scales with the number of magnetic moments. In order to reproduce the measured signal size of the paramagnetic contribution we need a Co concentration corresponding to a doping level of 5.9%. Accordingly most if not all Co atoms seem to be paramagnetic in this measurement of the total magnetic moment. The low field temperature dependence is close to a

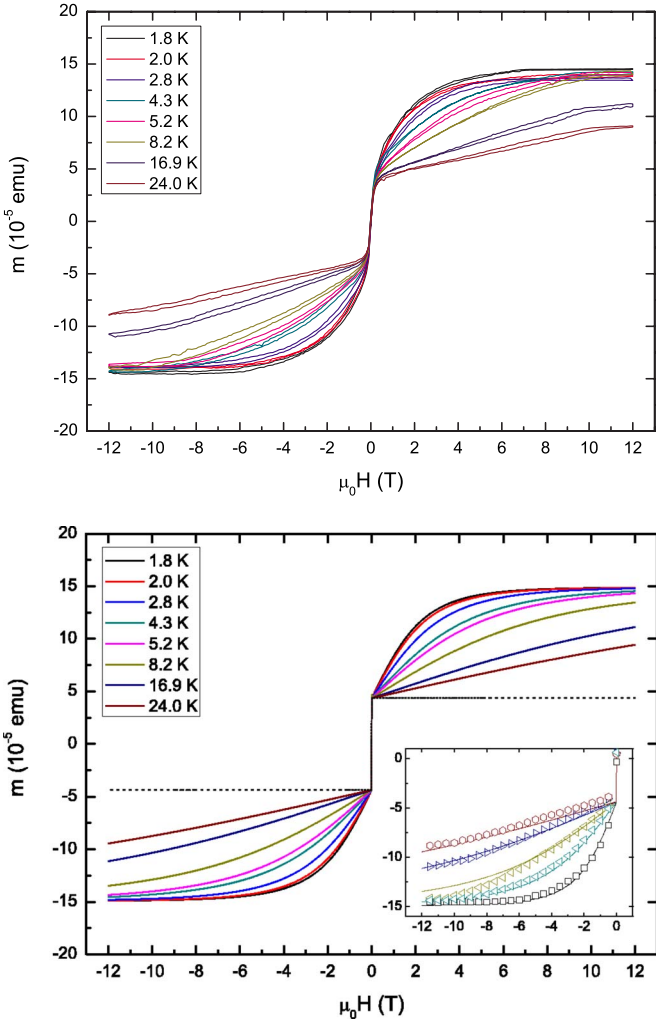

FIG. 4. (Color online) VSM data as measured (top) and simulated (bottom) for the same temperatures. The simulation shows the temperature independent ferromagnetic contribution separately as an additional dashed curve. The inset shows an overlay of the simulated and experimental data for selected temperatures.

Curie behavior (proportional to $1/T$), but close inspection of the low temperature data shows an improved agreement by an introduction of a small antiferromagnetic interaction between Co atoms with a Curie-Weiss temperature of $\Theta=-1$ K. This is in contrast to the strong antiferromagnetic interaction with $T_{\text{Néel}}=400$ K postulated by Kobayashi *et al.*[12] in order to explain the temperature independent paramagnetic susceptibility in their XMCD experiments. Our XMCD experiments discussed below show in agreement with the magnetization measurements also a strong temperature dependence, with a small Curie-Weiss temperature of $\Theta=30$ K. For thicker samples we observed stronger paramagnetic contributions, while the strength of the ferromagnetic contribution was fluctuating. We assume it could relate to the distorted film growth at the substrate interface, where defects are frequent. Possibly most of this part of the film shows defect induced ferromagnetism which was already supposed by Coey *et al.*[13] For undoped samples we did not see any ferromagnetism as expected, but a small paramagnetic contribution which seems not to come from the sub-

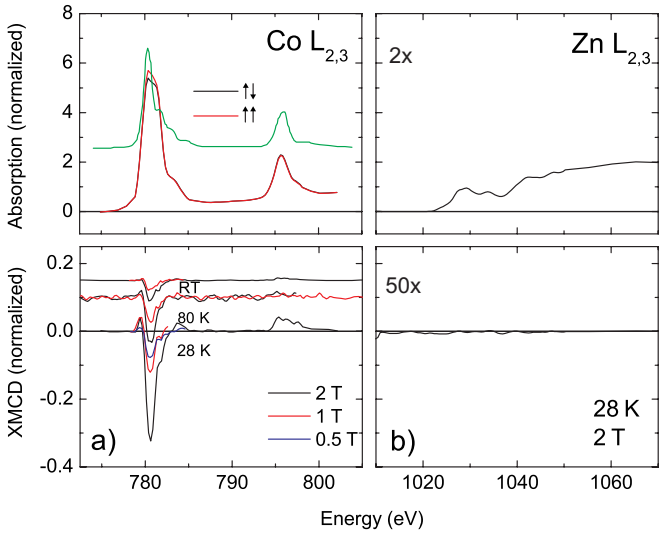

FIG. 5. (Color online) XAS and XMCD spectra at the Co $L_{2,3}$ and Zn $L_{2,3}$ edges of a 5% Co doped ZnO thin film sample.

strate, though we cannot exclude some paramagnetic impurities in the ZnO.

C. XMCD

In order to check the magnetic nature of the Co -atoms we performed x-ray magnetic circular dichroism measurements at the Co and Zn $L_{2,3}$ absorption edges. XMCD spectra were taken at normal incidence geometry. The extracted sum rule related magnetic moments have been normalized to the degree of circular polarization of 93±3%. All spectra are carefully background subtracted and edge normalized using the same background and normalization factor for parallel and antiparallel orientation of the photon beam k vector with respect to the sample magnetization. Further experimental details and data analysis have been published elsewhere.[14] Representative experimental XAS and XMCD spectra at the Co $L_{2,3}$ and the Zn $L_{2,3}$ edges of a 5% Co-doped ZnO thin film sample are shown in Fig. 5. The Co $2_p \rightarrow 3d$ absorption, probing the unoccupied Co $3d$ states, is shown in Fig. 5(a). The noise level of this small XMCD signal exhibits a visible temperature dependency, related to the evaporation of L-He and L-N, which is absent at room temperature (RT) spectra. The spectral shape of the resonant XAS lines [red (dark gray) and black] is quite different to typical metallic spectra.[15] For direct comparison we have reproduced in Fig. 5(a) [green (gray) curve] the theoretical multiplet spectrum of Co in tetrahedral coordination (from Ref. 16, Fig. 13, Co $3d^7$ configuration, T_d symmetry, and Dq=1.5 eV). The shape of our Co $L_{2,3}$ spectra is quite similar to the tetrahedral multiplet spectra. This provides a consistent description of Co ions located at the Zn site in tetrahedral coordination, as given by the crystal structure. For octahedral coordination, the theoretical XAS spectra (also in Ref. 16) are in much less agreement to the tetrahedral coordination, especially for the $3d^7$ configuration, which is the most likely one of diluted Co in ZnO. These results and the conclusion of tetrahedrally coordinated Co ions in a $3d^7$ configuration are in excellent agreement with other published experimental results and theoretical XAS calculations, supporting the n-type nonclustered Co $3d^7$ ion picture.[12,17] In the lower part of Fig. 5(a) the corresponding Co XMCD spectra are shown. The Co XMCD signal shows significant field and temperature dependent variations. While the XMCD signal is about to be proportional to the magnetic field, a strong decrease as a function of temperature could be observed. This observation is typical for paramagnetic materials and unexpected for a ferromagnetic system. This will be discussed on a quantitative basis below. Similar to the observation above, the spectral shape is clearly different to metallic Co spectra,[12,18] again indicating a weakly interacting environment providing multipletlike features different to metallic systems. Similar to the XAS spectra, the shape of the XMCD spectra also confirms the Co $3d^7$ ion picture, and is in good agreement to other XMCD results published so far.[12] This observation shows that no Co metal clusters are present in a significant amount. Figure 5(b) shows the Zn $L_{2,3}$ edge spectra, probing the unoccupied Zn $3d$ site. The resonance of the Zn $L_{2,3}$ XAS lines is very weak, indicating a Zn $3d^{10}$ configuration, as expected. The lower part of Fig. 5(b) shows the corresponding Zn $L_{2,3}$ XMCD, in an expanded view. No significant Zn XMCD signal could be observed, consistent to the nonresonant spectral line shapes of the corresponding XAS spectra shown above. This clearly demonstrates the absence of significant Zn $3d$ magnetism in doped ZnO. We will now focus on the quantitative discussion of the Co magnetic moments, which have been derived by the use of sum rules, using a number of holes n_h=3 consistent to the above discussed XAS and XMCD multiplet structure, which is consistent to the $3d^7$ configuration.[12,15,19,20] In an applied magnetic field of 2 T and at a temperature of 28 K, Co provides a projected $3d$ spin moment/ion of m_S=0.141μ_B, and an orbital projected moment of m_L=0.036μ_B (RT at 2 T: m_S=0.026μ_B, m_L =0.008μ_B). The spin values at both temperatures are quite close to a pure paramagnetic moment of a spin 3/2 system. In order to prove the paramagnetic behavior of Co, the field dependence of the Co XMCD signal has been monitored by measurements of the L_3 edge region between 778.5–782.8 eV and evaluating the total area below this XMCD peak. These area related values have been normalized to the sum rule derived spin moment from the full range measurements discussed before. The results are shown in Fig. 6 for three different temperatures and in applied fields up to 2 T. They indicate no ferromagnetic or remnant behavior for the Co atoms at all temperatures. In addition the temperature dependence has been measured in an applied field of 2 T, shown in the inset of Fig. 6. The spin moment follows a Curie law behavior $M_S(T)$=0.004μ_B+4.8 $\mu_B/(T/[\mathrm{K}]+30.5)$ with a Curie-Weiss temperature of −30.5 K, clearly indicating comparably weak antiferromagnetic coupling and no magnetic ordering. The absolute value of the non-temperature dependent Co magnetization has been estimated by a fit (shown in the inset of Fig. 6) to be $m_{S,\mathrm{const}}$ =0.004±0.004μ_B. No sign or indication for Co related ferromagnetism could be found, excluding Co related ferromagnetism as an origin for the observed ferromagnetism in this compound. However, the TEY mode sampling depth is about 5 nm, which clearly prevents the interface XMCD investiga-

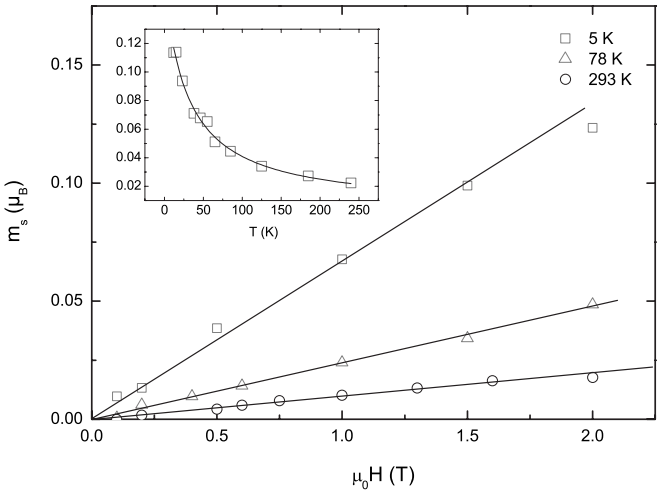

FIG. 6. Field-dependent Co XMCD magnetic moments for three different temperatures. The inset shows the temperature dependent Co XMCD magnetization and a corresponding Curie-Weiss law fit.

tion in TEY mode. By this method we can only exclude Co related ferromagnetism for the upper part of the film. But Co cluster formation at the interface to the substrate was not observed in the TEM investigation. We could also not detect secondary phases in x-ray diffraction. Summarizing the XMCD results, we have found only paramagnetic behavior of the Co 3*d* magnetism, down to low temperatures. This excludes Co atoms in the undistorted upper part of the ZnO film as the origin of the RT ferromagnetism. The constant ferromagnetic contribution in the VSM measurement would correspond to 1 Bohr magnetons per Co atom (at 5% nominal doping level). A ferromagnetic contribution of this size should be clearly visible at all temperatures in the XMCD measurements. However, the absolute Co XMCD related magnetization behavior shows no sign of saturation and is consistent to a pure paramagneticlike behavior at all measured temperatures. Due to higher temperatures and smaller fields in the XMCD experiment the Co absolute moments are up to two orders of magnitude smaller compared to magnetometry results (see above), but again in very good agreement to a model of paramagnetic Co ions. Our results are in strong contrast to other published XMCD results, which found a mixture of antiferromagnetically and ferromagnetically coupled Co ions.[12] We would like to emphasize that it is essential to have a very high signal to noise ratio present at the XMCD system, to measure paramagnetic and also strongly diluted magnetic moments at higher temperatures.

D. Transport properties

While a Co-derived magnetic impurity band was not found in the XMCD measurements, charge transport in such a magnetic impurity band should result in an anomalous Hall contribution. Therefore we investigated in detail magnetotransport properties of doped and undoped samples. The influence of magnetic impurities on the transport properties is distinct. Whereas there is a significant influence concerning the magnetoresistance, the Hall effect is hardly changing.

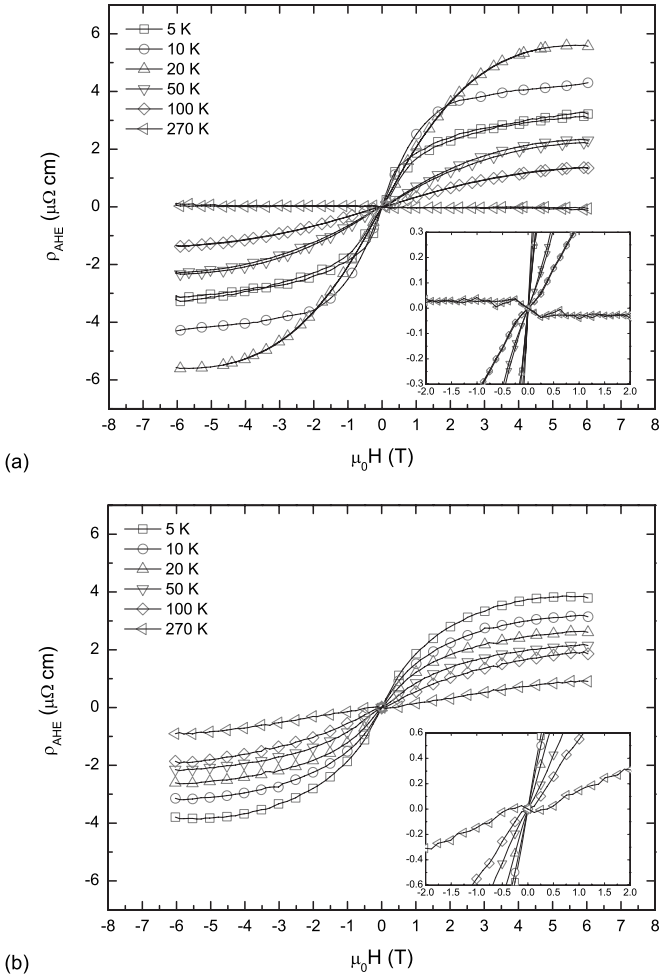

FIG. 7. Nonlinear Hall effect in $Zn_{0.95}Co_{0.05}O$ (a) and undoped ZnO (b). Doped and undoped samples exhibit a nonlinear Hall effect consisting of a strong high field contribution and a weak low field contribution. The effect seems to go with the magnetization. The data was generated by subtracting the high field slope (from 5 to 6 T) of the Hall effect.

The *R* vs *T* behavior of our samples is exponential as expected for a semiconductor. The charge carrier density which is calculated from the Hall data is as well exponential in temperature. At 300 K it is in a range of 1×10^{19}–3×10^{19} cm^{-3}, for both doped and undoped films. With 0.9 to 1.8 meV the activation energy is very low indicating a degenerate behavior. At first view there seems to be no anomalous Hall effect and the Hall resistivity looks simply linear with the applied field. Only a closer look reveals very small reproducible deviations from linear Hall behavior, which we denominate as anomalous contributions in the following. Surprisingly these nonlinear contributions are very similar in doped and undoped samples. They contribute about 3% of the normal effect and are shown in Fig. 7. To our knowledge there is only one other report about anomalous Hall effect in ZnCoO from Peng *et al.*,[21] which is probably due to the very small magnitude of the signal. Further data analysis shows that the effect consists of a high field and a very weak low field contribution. The high field contribution is up to 6 $\mu\Omega$ cm for doped and up to 4 $\mu\Omega$ cm for undoped ZnO,

whereas the low field one is below 0.1 $\mu\Omega$ cm for both. Because its saturation field of 0.5 T corresponds with that of the magnetometry data one is tempted to identify the small low field contribution to result from the ferromagnetism in ZnCoO. However, we could not detect ferromagnetic behavior in undoped samples. As ferromagnetic behavior was reported for other nondoped semiconductors,[22] a small ferromagnetic moment below our detection limit ($\approx 10^{-6}$ emu) might exist in the undoped film. Thus the origin of the low field contribution remains speculative. In the following we evaluate the much stronger high field deviations from the linear Hall behavior. For the high field contribution we did not find a scaling behavior $\sigma_{\mathrm{AHE}} \propto \sigma_{xx}^{n}$. This is in contrast to the findings of Toyosaki *et al.*,[23] who reported clear anomalous Hall behavior in Co doped TiO_2. Again the nondoped ZnO shows similar behavior. One possible explanation for the high field contribution in both doped and undoped ZnO is that the relative band occupation of different parts of the conduction band changes with magnetic field. This can lead to deviations from linear magnetic field dependence of the Hall conductivity. Our explanation is based on the theoretical background of the magnetoresistance results shown below. A similar behavior was also observed in manganites,[24,25] though in this case it is due to a magnetic field induced shift of the metal-insulator transition.

The transversal magnetoresistance was measured at various temperatures and for two different orientations of the magnetic field. In Fig. 8 we show the results for magnetic field perpendicular to the film plane. The magnetoresistance effect is strongly temperature dependent. While at low temperatures there is a positive and negative MR in a range of 0 to 6 T, at higher temperatures only a negative magnetoresistance is observed. The results are similar to that of Wang *et al.*[26] At low temperatures the MR is even changing its sign twice for Co doped ZnO. At 10 K the sign changes for $B = 1.5$ and 3.5 T while for 5 K it happens at 0.2 and 4.2 T. The curve profile is also very sensitive to the charge carrier density; there is a significant change in MR for carrier densities of 3.2×10^{19} cm^{-3} and 1.25×10^{19} cm^{-3} in our case. We also observed an anisotropy in transversal magnetoresistance with a difference in magnitude of 20% for in-plane and out-of-plane field orientation. For undoped ZnO with a similar charge density the negative contribution dominates, which could indicate a correlation between magnetic impurities and MR. Following the report of Reuss *et al.*[27] we used their semiempirical expression for the relative magnetoresistance, originally from Khosla *et al.*,[28] consisting of a negative and positive contribution to fit our data:

$$\Delta\rho/\rho_0 = -a^2 \ln(1 + b^2B^2) + \frac{c^2B^2}{1 + d^2B^2} \tag{1}$$

$$a^2 = A_1 J \rho_F [S(S+1) + \langle M^2 \rangle], \tag{2}$$

$$b^2 = \left[1 + 4S^2\pi^2\left(\frac{2J\rho_F}{g}\right)^4\right]\frac{g^2\mu^2}{(\alpha kT)^2}. \tag{3}$$

The negative component is explained by spin scattering taking in account the third order *s-d* exchange Hamiltonian

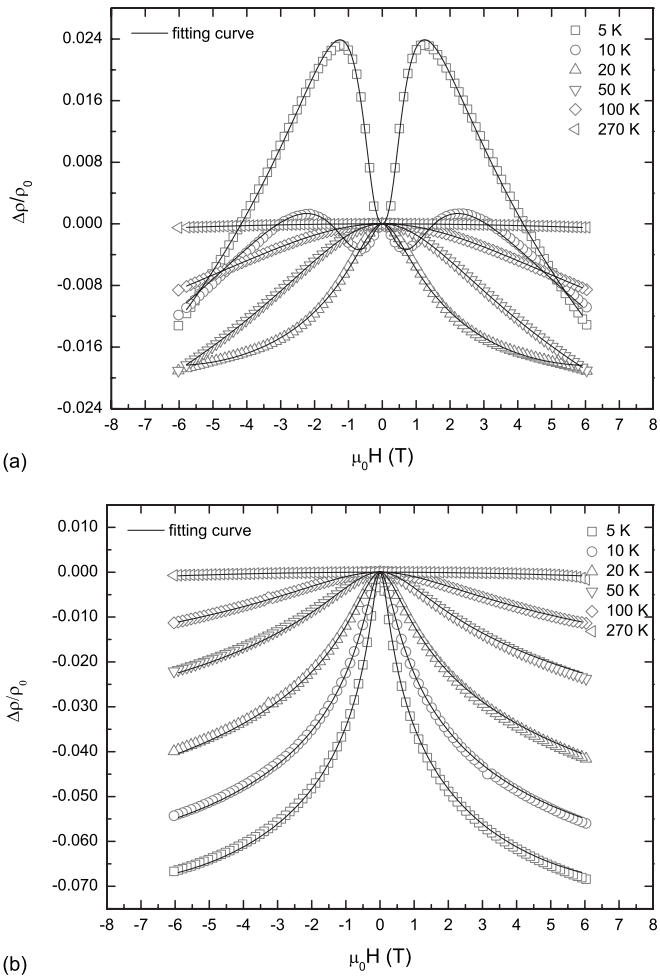

FIG. 8. Magnetoresistance in (a) $Zn_{0.95}Co_{0.05}O$ and (b) undoped ZnO (b). A positive and a negative component of the MR were observed. For doped samples this leads to sign changes at low temperatures. For undoped samples the negative contribution dominates.

while the positive one is due to a field induced change in the relative populations of two conduction bands with different conductivities which could also be an explanation for the unusual high field Hall effect as already mentioned above. The fitting parameters a and b depend on several properties as the average magnetization $\langle M \rangle$, the spin of the localized magnetic moments S, the exchange integral J, the density of states at the Fermi energy ρ_F, and A_1 as a measure for spin scattering. Parameters c and d are functions of conductivity and charge carrier concentration. Though Eq. (1) was actually meant for nonmagnetic degenerated semiconductors such as undoped ZnO, we show in the following that it also describes the MR behavior of TM doped ZnO films. As one can see the data can be well fitted with such an approach (Fig. 8). Parameters c and d yield a saturating positive high field MR. They are expected to change with the temperature because of the temperature dependent charge density. This positive magnetoresistance is compensated by the large negative contribution. Therefore both contributions are not independent in the fitting procedure. Nevertheless the least square fit parameters shown in Table I reveal clear tempera-

TABLE I. MR fit parameters for doped and undoped ZnO at various temperatures.

	T (K)	a	b	c	d
doped	5	0.13672	3.38956	0.47844	1.50142
	10	0.12354	1.85055	0.16992	0.65862
	20	0.09909	0.98132	0.03363	0.20608
	50	0.10186	0.59208	0.04472	0.4664
	100	0.11662	0.23123	0.01779	0.1557
	270	0.11221	0.09886	0.0104	0.06973
undoped	5	0.10194	5.54819	0.02205	0.26572
	10	0.09938	3.07206	0.01987	0.40929
	20	0.09856	1.62466	0.02467	0.38207
	50	0.10409	0.71064	0.03111	0.28104
	100	0.08998	0.42961	0.0197	0.22038
	270	0.1114	0.15822	0.01689	0.10945

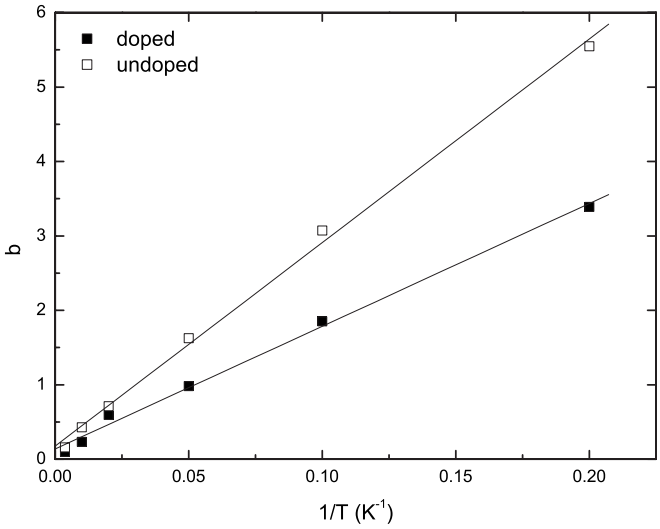

FIG. 9. b parameter vs inverse temperature.

ture dependencies of the fit parameters. Here we want to discuss the negative scattering contributions a and b of Eqs. (2) and (3), respectively. Regarding the temperature dependence of the parameters a and b (Table I) there is indeed a clear $1/T$ linearity of the parameter b, which is shown explicitly in Fig. 9, while the parameter a is more or less constant as expected from the definition. Comparing the doped and undoped sample one can see an evident change in the slope of the $b(1/T)$ relation in Fig. 9, whereas parameter a is changing only a little (Table I). Because the negative contribution is due to spin scattering, it contradicts expectations to find the negative component smaller for magnetically doped than for undoped samples.

Our comparative transport measurements on doped and undoped samples yield surprising results. A comparable nonlinear Hall signal is observed in both cases. The low temperature MR looks different for doped and undoped samples, however, the spin dependent magnetoresistive contribution was found to be smaller for the doped samples. Thus the Co-dopand atoms seem not to be strong scattering centers for conduction electrons.

IV. SUMMARY AND CONCLUSION

Structural, magnetic, and transport properties of 5% Co-doped and undoped ZnO films prepared by PLD were investigated. Doped samples exhibit ferromagnetic and paramagnetic behavior. Element specific magnetization measurements using XMCD showed purely paramagnetic behavior for the Co atoms and only nonmagnetic Zn atoms. The ferromagnetic contribution seems to have its origin in the first distorted atomic layers, for thicker films the paramagnetic contribution is dominant. Transport measurements show a small nonlinear Hall effect. Low field as well as high field contribution of the nonlinear Hall effect were observed. Undoped samples show a similar effect though they should not have any magnetic impurities. The high field contribution may have its origin rather in a magnetic field dependent band filling, while the origin of the low field contribution remains unclear. The magnetoresistance of the doped samples consists of a negative and a positive component leading to a double sign change at low temperatures. For undoped ZnO the negative contribution dominates the magnetoresistance. Our results could be fit with an approach that presumes spin scattering for the negative and a two-band model for the positive contribution. For undoped samples the negative spin scattering component is stronger than for doped samples pointing to a low interaction strength of the paramagnetic Co atoms with the conduction bands of the ZnO. Our XMCD, magnetization, and transport measurements show no indication that the magnetism in this oxidic diluted magnetic semiconductors has its origin in the magnetism of Co-dopant atoms including clusters or secondary phases. We presume rather defects in the base material induced by the dopants and/or defects at the film substrate interface are responsible for the observed ferromagnetism. Such unexpected ferromagnetism has already been reported in HfO_2 (Ref. 22) and Sc doped ZnO (Ref. 4) pointing to an occurrence of magnetic moments in oxides without partially filled shells.

ACKNOWLEDGMENTS

We would like to thank BESSY 2 PM3 beamline staff, especially T. Kachel, for support and help during the beamtime. This work was partially performed at and supported by BESSY. Additional financial support by Materials Research Center Mainz and the Max-Planck Society is gratefully acknowledged.

[1] H. Ohno, A. Shen, F. Matsukura, A. Oiwa, A. Endo, S. Katsumoto, and Y. Iye, Appl. Phys. Lett. **69**, 363 (1996).
[2] H. Ohno, D. Chiba, F. Matsukura, T. Omiya, E. Abe, T. Dietl, Y. Ohno, and K. Ohtani, Nature (London) **408**, 944 (2000).
[3] T. Dietl, H. Ohno, F. Matsukura, J. Cibert, and D. Ferrand, Science **287**, 1019 (2000).
[4] M. Venkatesan, C. B. Fitzgerald, J. G. Lunney, and J. M. D. Coey, Phys. Rev. Lett. **93**, 177206 (2004).
[5] K. Rode, A. Anane, R. Mattana, and J.-P. Contour, J. Appl. Phys. **93**, 7676 (2003).
[6] S. W. Jung, S.-J. An, and Gyu-Chul Yia, Appl. Phys. Lett. **80**, 4561 (2002).
[7] Y. Matsumoto, M. Murakami, T. Shono, T. Hasegawa, T. Fukumura, M. Kawasaki, P. Ahmet, T. Chikyow, S. Koshihara, and H. Koinuma, Science **291**, 854 (2001).
[8] Z. Jin, T. Fukumura, and M. Kawasaki, Appl. Phys. Lett. **78**, 3824 (2001).
[9] S. B. Ogale, R. J. Choudhary, J. P. Buban, S. E. Lofland, S. R. Shinde, S. N. Kale, V. N. Kulkarni, J. Higgins, C. Lanci, J. R. Simpson, N. D. Browning, S. Das Sarma, H. D. Drew, R. L. Greene, and T. Venkatesan, Phys. Rev. Lett. **91**, 077205 (2003).
[10] M. Ivill, M. E. Overberg, C. R. Abernathy, D. P. Norton, A. F. Hebard, N. Theodoropoulou, and J. D. Budai, Solid-State Electron. **47**, 2215 (2003).
[11] J. M. D. Coey, M. Venkatesan, and C. B. Fitzgerald, Nat. Mater. **4**, 173 (2005).
[12] M. Kobayashi, Y. Ishida, J. l. Hwang, T. Mizokawa, A. Fujimori, K. Mamiya, J. Okamoto, Y. Takeda, T. Okane, Y. Saitoh, Y. Muramatsu, A. Tanaka, H. Saeki, H. Tabata, and T. Kawai, Phys. Rev. B **72**, 201201(R) (2005).
[13] J. M. D. Coey, J. Appl. Phys. **97**, 10D313 (2005).
[14] E. Goering, S. Gold, A. Bayer, and G. Schuetz, J. Synchrotron Radiat. **8**, 434 (2001).
[15] C. T. Chen, Y. U. Idzerda, H.-J. Lin, N. V. Smith, G. Meigs, E. Chaban, G. H. Ho, E. Pellegrin, and F. Sette, Phys. Rev. Lett. **75**, 152 (1995).
[16] G. van der Laan and I. W. Kirkman, J. Phys.: Condens. Matter **4**, 4189 (1992).
[17] J. Okabayashi, K. Ono, M. Mizuguchi, M. Oshima, Subhra Sen Gupta, D. D. Sarma, T. Mizokawa, A. Fujimori, M. Yuri, C. T. Chen, T. Fukumura, M. Kawasaki, and H. Koinuma, J. Appl. Phys. **95**, 3573 (2004).
[18] S. S. Dhesi, H. A. Dürr, G. van der Laan, E. Dudzik, and N. B. Brookes, Phys. Rev. B **60**, 12852 (1999).
[19] B. T. Thole, P. Carra, F. Sette, and G. van der Laan, Phys. Rev. Lett. **68**, 1943 (1992).
[20] P. Carra, B. T. Thole, M. Altarelli, and X. Wang, Phys. Rev. Lett. **70**, 694 (1993).
[21] Y. Z. Peng, T. Liew, and T. C. Chong, Appl. Phys. Lett. **88**, 192110 (2006).
[22] M. Venkatesan, C. B. Fitzgerald, and J. M. D. Coey, Nature (London) **430**, 630 (2004).
[23] H. Toyosaki, T. Fukumara, Y. Yamada, K. Nakajima, T. Chikywo, T. Haseguwa, H. Koinuma, and M. Kawasaki, Nat. Mater. **3**, 221 (2004).
[24] G. Jakob, F. Martin, W. Westerburg, and H. Adrian, Phys. Rev. B **57**, 10252 (1998).
[25] Y. Lyanda-Geller, S. H. Chun, M. B. Salamon, P. M. Goldbart, P. D. Han, Y. Tomioka, A. Asamitsu, and Y. Tokura Phys. Rev. B **63**, 184426 (2001).
[26] J. Wang, Z. Gu, M. Lu, D. Wu, C. Yuan, S. Zhang, Y. Chen, S. Zhu, and Y. Zhu, Appl. Phys. Lett. **88**, 252110 (2006).
[27] F. Reuss, S. Frank, C. Kirchner, R. Kling, and Th. Gruber, Appl. Phys. Lett. **87**, 112104 (2005).
[28] R. P. Khosla and J. R. Fischer, Phys. Rev. B **2**, 4084 (1970).